Article:
Zhang, M, Bi, C, Xia, Y et al. (7 more authors) (2023) Water-Driven Synthesis of Deep-Blue Perovskite Colloidal Quantum Wells for Electroluminescent Devices. Angewandte Chemie, 62 (12). e202300149. ISSN 0044-8249

https://doi.org/10.1002/anie.202300149

Supporting Information

Water-Driven Synthesis of Deep-Blue Perovskite Colloidal Quantum Wells for Electroluminescent Devices

Mengqi Zhang[+], Chenghao Bi[+], Yuexing Xia, Xuejiao Sun, Xingyu Wang, Aqiang Liu, Shuyu Tian, Xinfeng Liu, Nora H. de Leeu, Jianjun Tian[*]

M. Zhang, Dr. C. Bi, A. Liu, S. Tian, Prof. J. Tian
Institute for Advanced Materials and Technology
University of Science and Technology Beijing
Beijing 100083, China
and
Shunde Innovation School
University of Science and Technology Beijing
Foshan, Guangdong, 528399, China
[*]E-mail: tianjianjun@mater.ustb.edu.cn
Y. Xia, Prof. X. Liu
CAS Key Laboratory of Standardization and Measurement for Nanotechnology
Beijing National Center for Nanoscience and Technology
Beijing, 100190, China
and
University of Chinese Academy of Sciences
Beijing, 100049, China
Dr. X. Sun
Institute of Semiconductors Chinese Academy of Sciences
Beijing, 100083, China.
X. Wang, Prof. N. H. de Leeu
School of Chemistry
University of Leeds
Leeds, LS2 9JT, UK.
[+] These authors contributed equally to this work.

Author Contributions

J. T. designed the experiments and supervised the project. M.Z. and C.B. performed the QWs synthesis and characterization of the device. Y.X. and X.L. analyzed the TA spectra of the QWs. X. W. and N.H.d.L. contributed to the DFT calculations. A.L. conducted the performance optimization of the perovskite LEDs. M.Z. and S.T. finished the temperature-dependent PL measurement. M.Z. and X.S conducted the characterization of optical properties. M.Z. and Y.X. organized the data and wrote the manuscript. J.T., N.H.d.L., and X.L. provided revisions to the manuscript. All authors reviewed and contributed to the final manuscript

Experimental section

Materials

Cesium carbonate (Cs_2CO_3, alfa 99.9%,), lead (II) bromide ($PbBr_2$, youxuan 99.9%), 1-octadecene (ODE, alfa tech.90%), oleic acid (OA, alfa tech.90%), oleylamine (OAm, Aladdin tech.90%), phenylethylamine (PEA, Sigma-Aldrich 90%), didodecylamine (DDDAM, TCI 97%), methyl acetate (MeOAc, Aladdin anhydrous 99.5%), ethyl acetate (Aladdin anhydrous 99.5%), and hexane (Aladdin analytical reagent 97%), and water (purified water) were purchased and used as received without any further purification.

Synthesis of Cs-oleate

Cs_2CO_3 (0.1g), OA (700 μl), and ODE (10 ml) were loaded into three-necked flasks (100 ml) and dried under vacuum at 100℃ for 1 h. Subsequently, the mixture was heated to 120℃ and continued heating for 15 minutes, followed by pumping N_2 into the flask. This process was repeated 3 times to completely remove water or oxygen. Till now, a colorless and clear Cs-Oleate solution could be obtained. Keep the solution at 105 ℃ before injection.

Synthesis of the pristine $CsPbBr_3$ QWs

The pristine sample was prepared through a conventional hot-injection method. A 100 ml three-necked round flask with 10 ml ODE and 0.138 g $PbBr_2$ was placed in a heating agitator, which was gradually heated to 100 ℃ in a vacuum for degassing for 1 h. Then the temperature was increased to 120 ℃ and continued heating for 15 minutes, followed by the N_2 flow being switched into a flask three times, and kept flowing constantly. After pumping N_2, 0.6 ml OAm and 1.2 ml OA pre-heated at around 60 ℃ were quickly injected into the mixture. At this time, the solution became clear without bubble generation. The temperature was decreased to 105 ℃ and kept steady for a while. At this stage, 1.6 ml Cs-oleate precursor solution was quickly injected into the flask and placed the flask into an ice bath to terminate the reaction.

Preparation of the WD-synthesized QWs

During the synthesis of QWs, the first-stage synthesis process was the same as it of the pristine sample. The difference was that after the cooling stage, the flask was put back

to the heating agitator at the temperature at 70 ℃. 40 μL water was introduced into the as-synthesized QWs solution at this temperature, stirring for about 30s.

Purification process

Both QWs were purified by mixing with MeOAc (volume ratio 2.5:1) and then centrifugation at 8000 rpm for 5 min. The product was dried and redispersed in octane for storage. For device fabrication, we conducted the purification process for the second time. The ratio of hexane/ethyl acetate mixed solvents to QWs solution is recommended to be 1.5 to 1 for the second purification process. The centrifugation is set to be at 12000 – 15000 rpm for about 5 minutes.

Ligand exchange for QWs

To successfully prepare LEDs, a ligand exchange strategy has been adopted. Still, based on the pristine solution, 20 μL DDDAM in toluen (concentration is 0.5M) was injected into the flask after introducing the water. Note: some white precipitates might occur at the bottom of the flask, indicating the dissolution of perovskite, so the DDDAM should be added quickly. After that, 8 μL PEA was also added into the colloidal solution to ligand exchange under stirring for a few minutes. The final obtained $CsPbBr_3$ QWs were separated by MeOAc and centrifugation and then redissolved in hexane.

Fabrication of QWs-based LEDs

Prepatterned ITO glasses were ultrasonically washed with detergent solution, deionized water, acetone, and ethanol. After the washing process, the substrates were dried with compressed N_2 flow. The substrates were placed into a UV-Ozone cleaner (Novascan, PSD) for 15 min. Commercial PEDOT: PSS solution (Baytron PVP Al 4083) filtered through a 0.45μm N66 filter was spin-coated onto the ITO glass substrates at 3500 rpm for the 60s and annealed at 140℃ for 10 min. The PEDOT: PSS-coated substrates were swiftly transferred into a glovebox filled with N_2. These samples were annealed at 140℃ for 5 mins with the N_2 flow. Commercial PVK (Xi'an Polymer Light Technology Corp) in chlorobenzene solution (4 mg/ml) was deposited on the PEDOT: PSS layer by spin coating at 2500 rpm for 45 s in a nitrogen-filled glovebox. These were subsequently annealed at 130℃ for 25 min under the constant N_2 flow. Perovskite QWs solution (~10 mg/ml, octane) was spin-coated onto the PVK layer at 2000 rpm for 45 s and then

annealed at 90 ℃ for 5 mins. The ZnO nanoparticles ethanol/isopropanol solution (25 mg/ml) was spin-coated onto the QWs layer at 2000 rpm for 45 s and then annealed at 100 ℃ for 10 mins (Note: This process should be carried out quickly to avoid the degradation of QWs layer caused by ethanol; the annealing period might be varied when the thickness of the QWs varies). Finally, Ag electrode (100 nm) was deposited on the ZnO layer by a thermal evaporation system.

Characterization

The XRD spectra of the pristine and WD-synthesized QWs were obtained by a MXP21VAHF X-ray diffractometer using Cu Kα radiation (λ = 1.5418 Å). UV-vis absorption spectra were obtained by a Shimadzu UV-3600 Plus spectrophotometer. PL spectra of the pristine and WD-synthesized QWs were obtained by a Guangdong F-280 fluorescence spectrometer. Time-resolved PL decay spectra of QWs were obtained by a Horiba Fluorolog spectrometer coupled with a 375 nm, 45 ps pulsed laser, and a time-corrected single-photon counting system. PLQYs were obtained by an integrating sphere (Edinburgh, FLS920). TEM and HRTEM of QWs were obtained by a JEOL JEM-2010 microscope operated at 200 kV. XPS spectra of the pristine and WD-synthesized QWs were tested by a PHI 5000 Versa Probe III spectrometer using a monochromatic Al Kα radiation source (1486.6 eV). FTIR spectra of the pristine and WD-synthesized QWs were obtained by a Varian 3100 FTIR spectrometer. The EL spectra and luminance–current density–voltage curves of QWs-based LEDs were collected by a Keithley 2400 source, a calibrated luminance meter, and a PR-655 Spectra Scan spectrophotometer (Photo Research).

Device characterization

The properties of LEDs were performed at room temperature. A Keithley 2400 source meter a calibrated luminance meter, and a PR-655 Spectra Scan spectrophotometer (Photo Research) were used for the measurements. The devices were operated with voltage from 1 V to 10 V with a step voltage of 0.2 V.

Data collection of in-situ PL profiles for the pristine and WD-synthesized QWs

The in-*situ* PL tracking system detected basic optical properties including PL intensity, FWHM, and wavelength variations during the synthesis process. With a UV lamp

(emission wavelength at 365 nm), PL spectra could be monitored via an optical fiber connected to the computer and recorded based on a 0.01s time interval. Data was collected after terminating the growth of QWs and putting the flask back into the heating sleeve under the string at 70 ° C for the 20s.

DFT Model establish and calculation

Taking the Cs-Br surface as the dominant possible termination surface when establishing the model, and assuming that the surface is saturated with H atoms to prevent possible magnetization in the system. we investigated the surface properties of common low-index surfaces such as (100), (110) and (111) surfaces of cubic $CsPbBr_3$. In this study, we have employed the Vienna Ab initio Simulations Package, VASP (version 5.4.4), to carry out all DFT calculations, where the projector-augmented wave method (PAW) was used to describe the ion−electron interaction and the exchange−correlation interaction was described through the generalized gradient approximation (GGA) with the Perdew−Burke−Ernzerhof (PBE) density functional. We have treated the following as valence electrons: Cs(5s5p6s), Pb(5d6s6p), I(5s5p), Br(4s4p), Zn(3d4s), C(2s2p), N(2s29) and H(1s). In addition, the kinetic energy cutoff for the plane-wave basis was set at 400 eV. The non-dipolar (010) surface was obtained using METADISE.30 code, where we have added a vacume of 15 Å along z direction and 6 × 6 × 6 and 4 × 4 × 1 centered Monkhorst Pack grids were used for the simulation of the bulk and surface slabs with adsorbates. Especially, in each surface model, there are 8 layers along z direction and we have fixed the 4 bottom layers and allow the rest to relax to mimic the real situation and, in this process, the London dispersion interactions was depicted through using the D3 van der Waals correction. All calculations of the bulk and surfaces reactions were performed with the conjugate gradient's method with a convergence criterion of 10^{-5} eV and 0.01 eV/Å for the electronic and ionic self-consistence respectively. In the calculations of surfaces, the adsorption energy was obtained through the equation:

$$E_{ad} = E_{sur+adsorbate} - E_{sur} - E_{adsorbate}$$

Where $E_{sur+adsorbate}$ is the total energy of adsorption model, E_{sur} is the total energy of surface and $E_{adsorbate}$ is the total energy of adsorbate.

Temperature-dependent PL measurement and calculation

The Arrhenius fitting of the integrated PL intensity of the pristine and WD-synthesized QWs by the following equation:

$$I\,(T) = \frac{I_0}{1 + Aexp(-\frac{E_b}{kT})}$$

Where I_0 is integrated PL intensity at 0 K, A is the proportional constant, E_b is the exciton binding energy, and k is the Boltzmann constant in eV.

Ultrafast femtosecond transient absorption (TA) measurement

Transient absorption spectra of samples were obtained using a commercial femtosecond pump-probe system (Helios, Ultrafast Systems). The pump beam was acquired by coupling the 800 nm, 1kHz amplified Ti: sapphire laser system (Astrella, Coherent) with the output of an optical parametric amplifier (Opera Solo, Coherent). The wavelength was able to scan from 360 to 800 nm. A mechanical chopper modulated the pump beam at a frequency of 500 Hz. The white light continuum probe beam from 415 to 620 nm (2 to 2.99 eV) was acquired by focusing a small part of the fundamental 800 nm beam on a CaF2 window. Finally, considering the instrument response function of this system, the system had an ultimate temporal resolution of approximately 150 fs.

Descriptions of the ligand-exchanged QWs

Ligand-exchanged QWs were characterized to present enhanced PL QY (near unity, 99%), reduced surface defects, and improved optical stability. These ligand-exchanged QWs gave an emission wavelength of 452 nm with a narrow FWHM of 20 nm. The similar emission wavelength and FWHM profile confirm that the water-driven ligand exchange does not influence the basic optical property of QWs, which is the foundation for any application. Besides, the PLQY is near unity which is around 99%. This great optical performance of ligand-exchanged QWs benefits from the great crystallinity and surface defect passivation. The reduction of surface defect density can be supported by the Time-resolved PL decay (TR PL) and Ultrafast femtosecond transient absorption

(TA) measurement. The average PL lifetime of the ligand-exchanged QWs was 3 ns, longer than that of the pristine QWs (~ 2.6 ns). The ligand-exchanged QWs have a faster radiative rate (0.36 ns^{-1}) and suppressed non-radiative rate (0.02 ns^{-1}), compared with the pristine counterpart (0.17 ns^{-1} and 0.21 ns^{-1}, correspondingly), indicating that non-radiative recombination in the ligand-exchanged QWs is eliminated through efficient surface defect reduction. From TA results, the ligand-exchanged QWs show enhanced and narrower ground-state bleaching (GSB) in comparison with the pristine QWs and the WD-synthesized QWs, which is attributed to the decrease of trap density for the WD-synthesized QWs. The spectral diffusion of the ligand-exchanged QWs is suppressed with time, indicating the trap density is reduced and confirmed by the higher PLQY of the ligand-exchanged QWs. The spectrum shape of the ligand-exchanged QWs remains almost unchanged for 5 ns with negligible redshift, which indicates the stability of these QWs. Besides, the ligand-exchanged QWs present single-exponential decay dynamics, revealing that the non-radiative recombination paths are effectively suppressed, and excited carriers are efficiently utilized. Thanks to the high performance of ligand-exchanged QWs, the LEDs can be well processed.

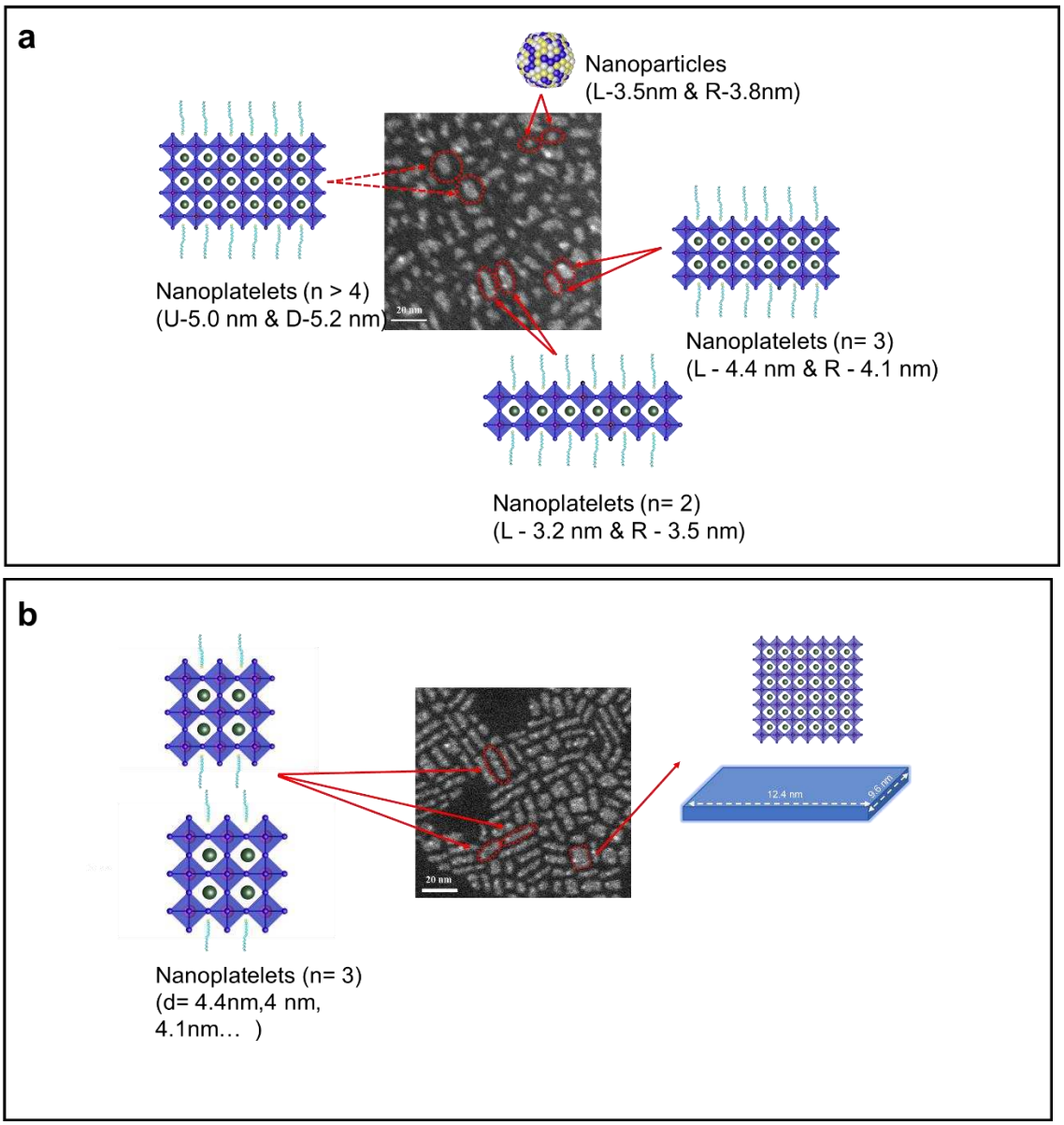

Figure S1. Size illustration of the (a) pristine QWs and (b) QWs with adding water for 15s.

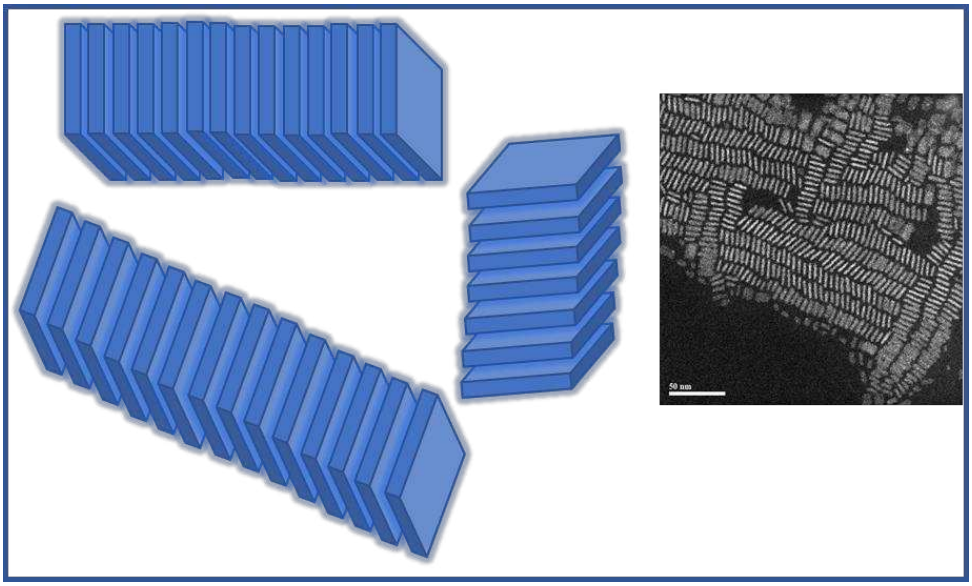

Figure S2. Illustration of the arrangement of the WD-synthesized QWs based on the HRTEM.

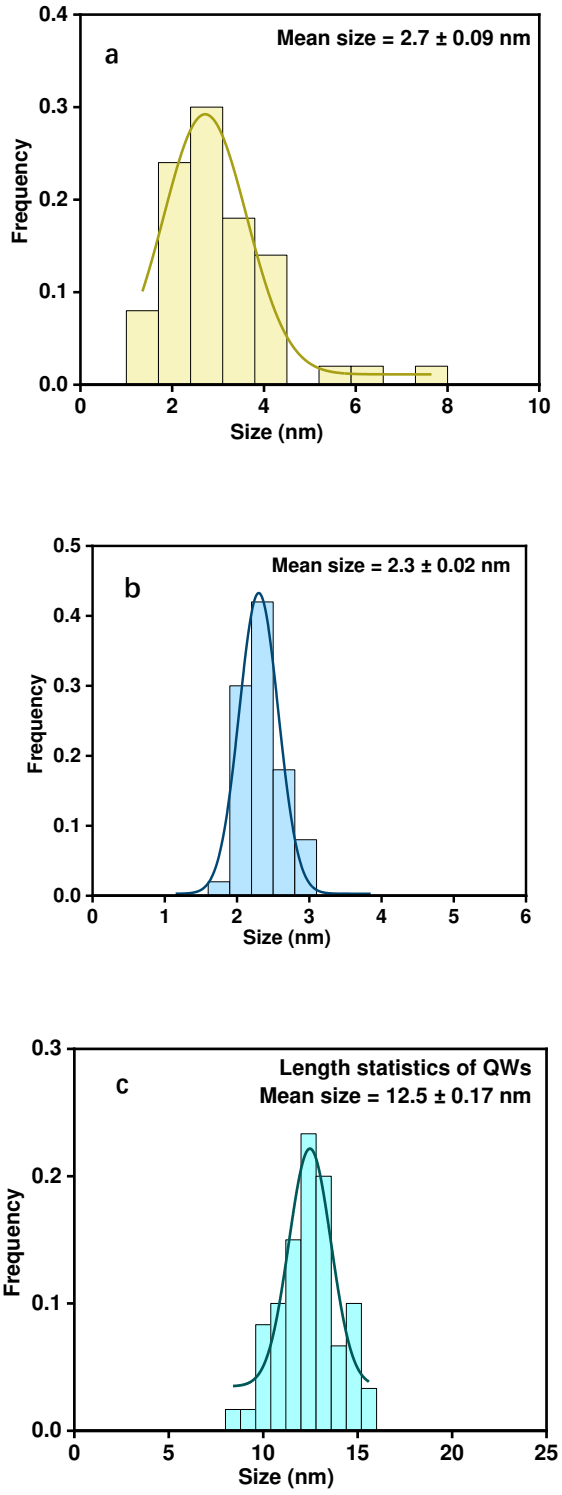

Figure S3. (a) Size distribution of the pristine QWs. (b) The thickness and (c) length statistics of the WD-synthesized QWs.

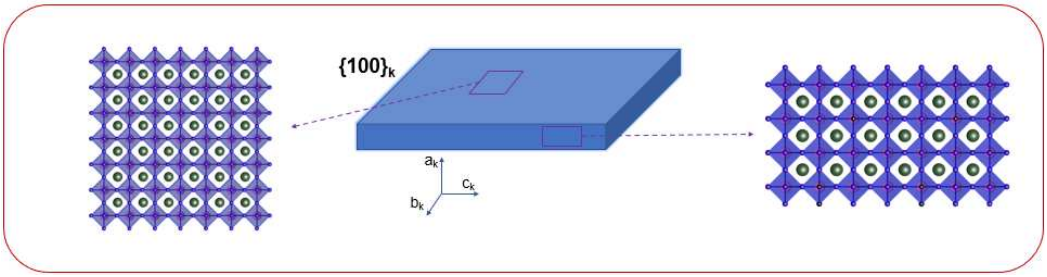

Figure S4. Illustration of the shape and structure of the WD-synthesized QWs.

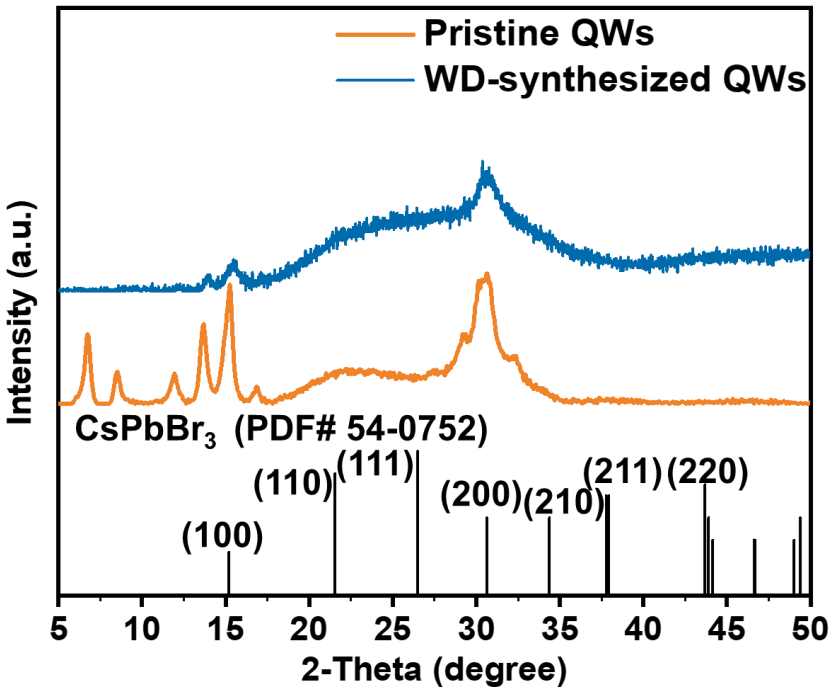

Figure S5. XRD profiles of the pristine and WD-synthesized QWs.

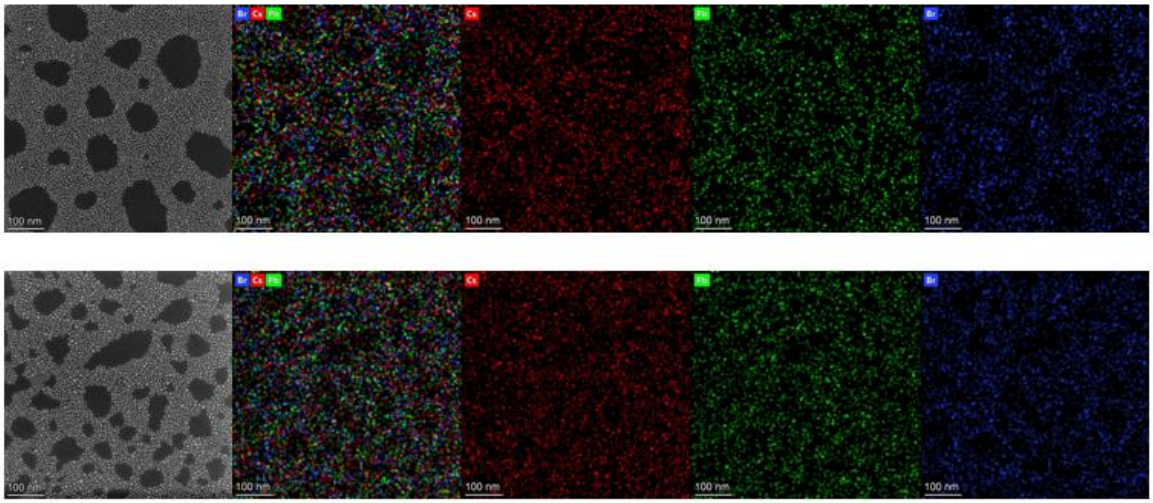

Figure S6. Elemental mapping of the pristine QWs (Upper) and WD-synthesized QWs (Down).

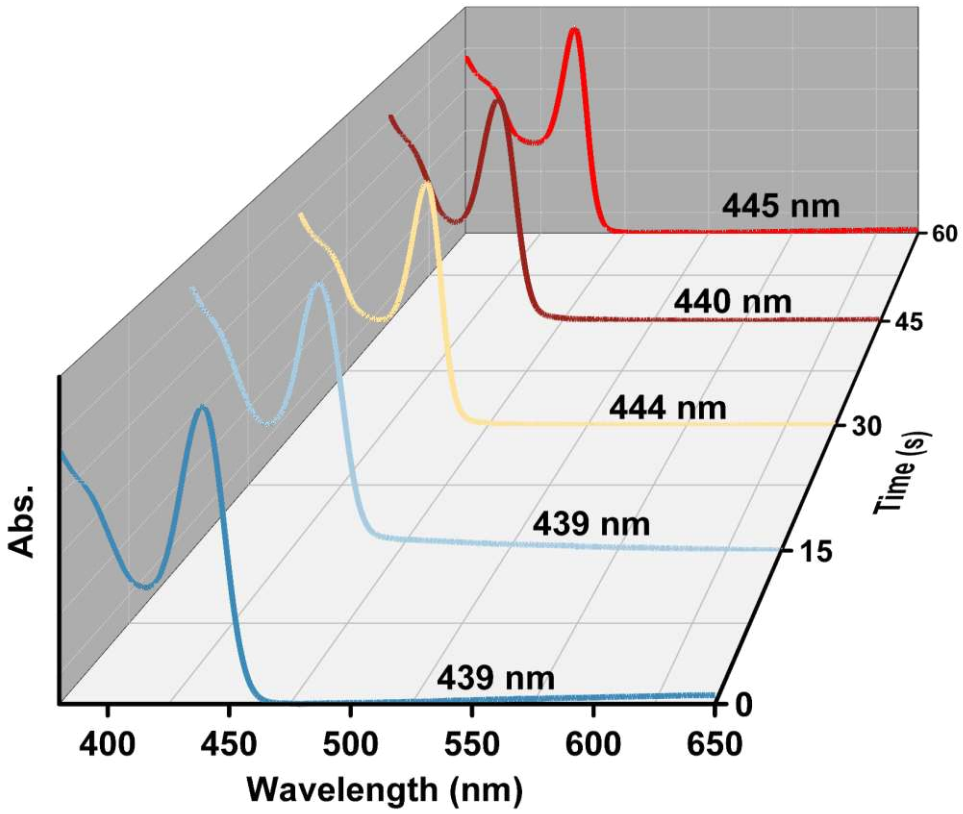

Figure S7. UV/Vis spectra of the WD-synthesized QWs with adding water at different stages (0 s, 15 s, 30 s, 45 s, and 60 s, respectively).

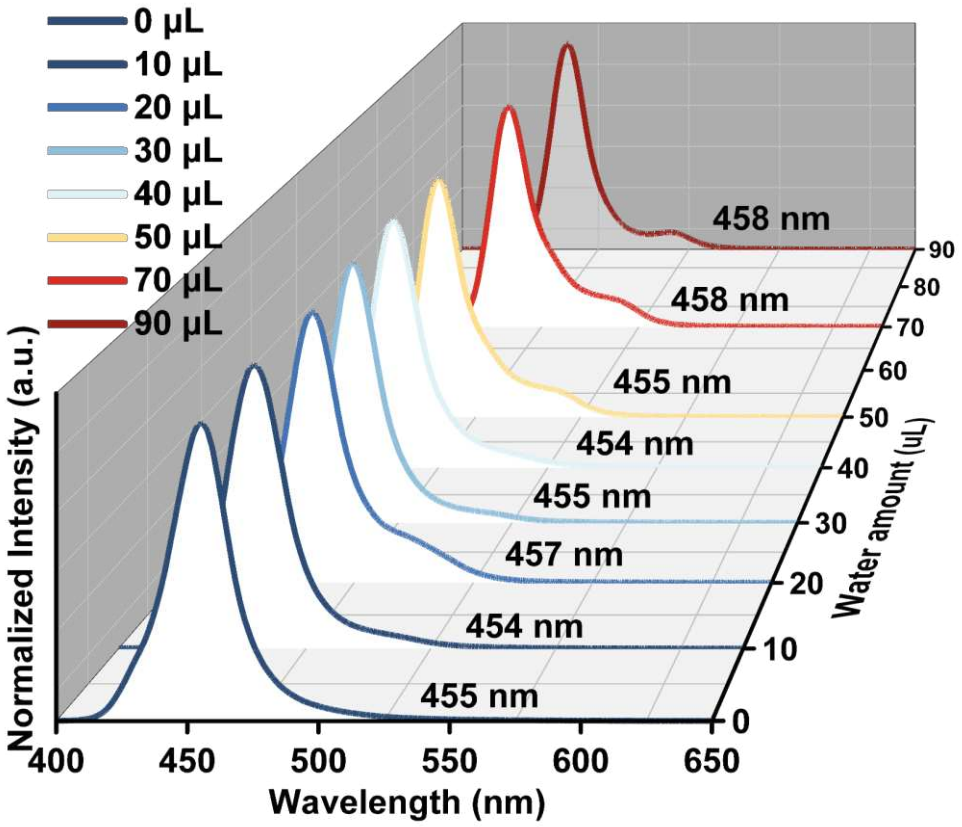

Figure S8. PL profile of the WD-synthesized with various water addition of 0, 10, 20, 30, 40, 50, 70, and 90 µL, respectively.

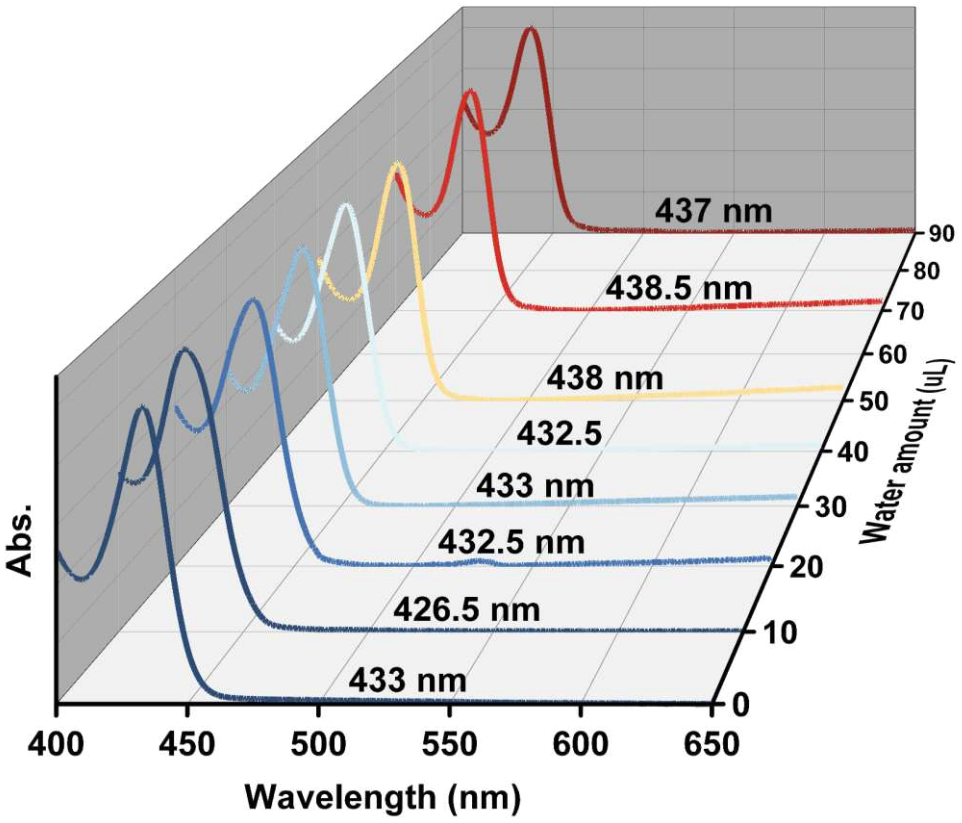

Figure S9. UV/Vis spectra of the WD-synthesized with various water addition of 0, 10, 20, 30, 40, 50, 70, and 90 μL, respectively.

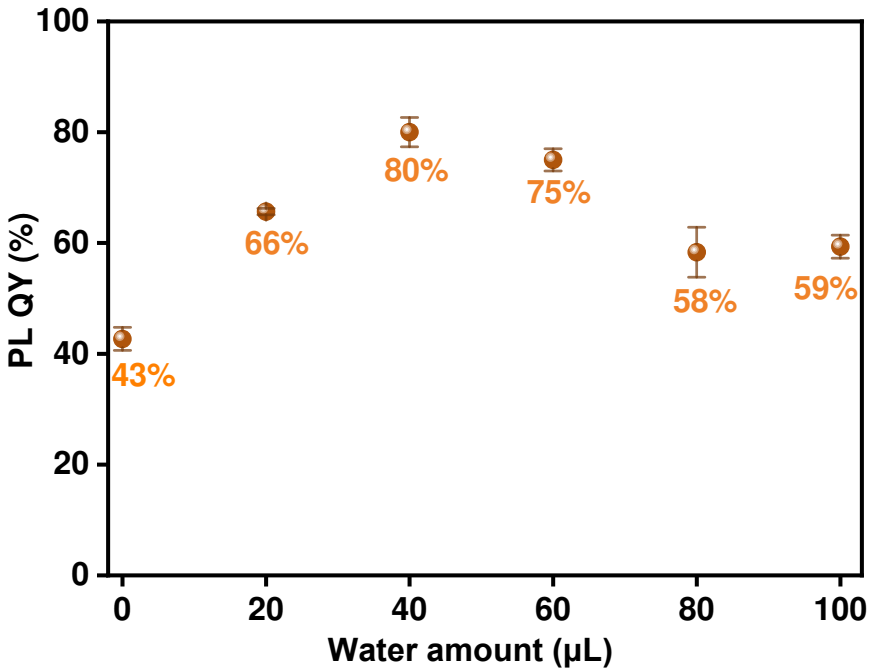

Figure S10. FWHM of the WD-synthesized with various water addition of 0, 10, 20, 30, 40, 50, 70, and 90 μL, respectively.

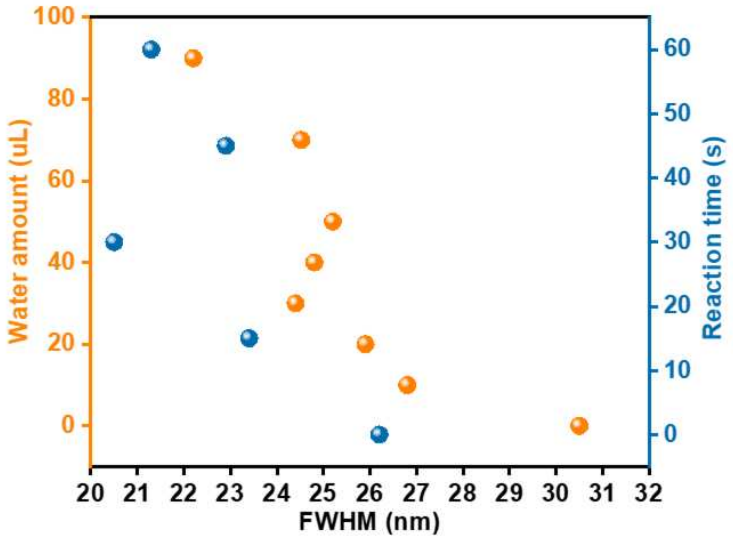

Figure S11. Average FWHM statistic of QWs by varying experimental conditions. Condition 1 (Yellow ball): Water addition of 0 uL, 20 uL, 40 uL, 60 uL, 80 uL and 100 uL without reaction time. Condition 2 (blue ball): water addition of 40 uL with reacting 0s, 15s, 30s, 45s and 60s, respectively.

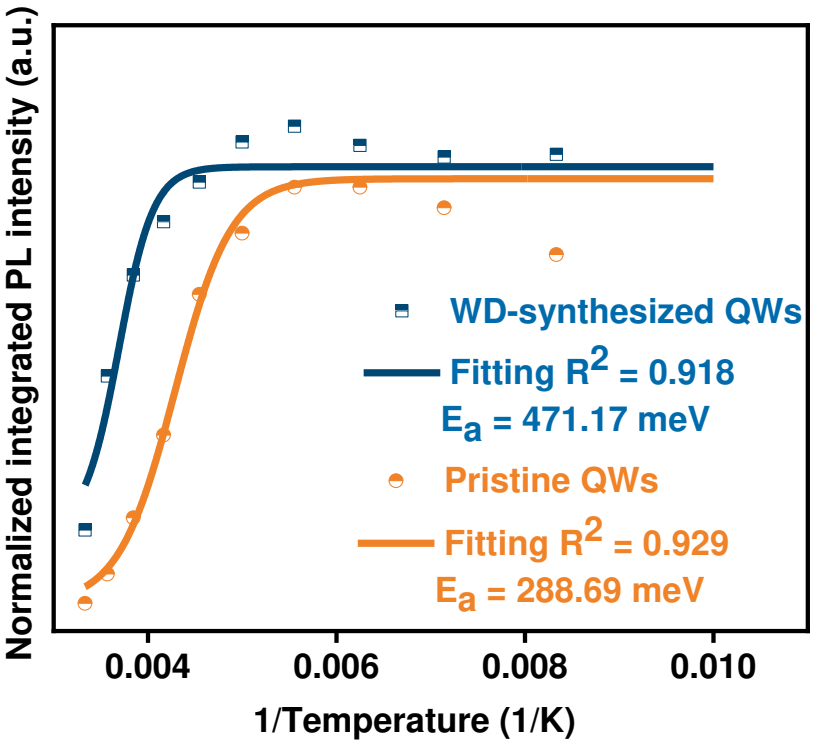

Figure S12. The temperature-dependent integrated PL intensity of the pristine and WD-synthesized QWs.

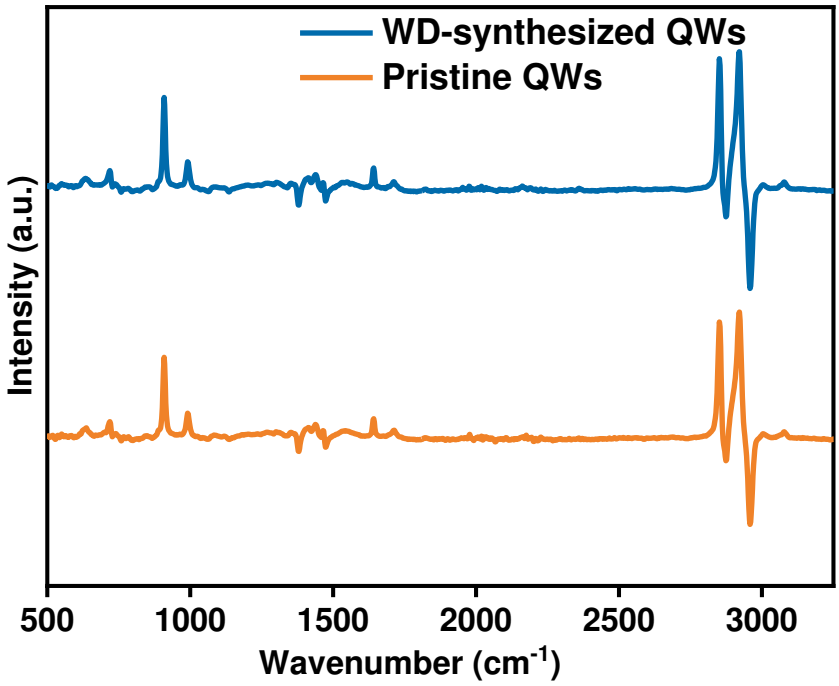

Figure S13. FTIR absorption spectra of the pristine and WD-synthesized synthesized QWs.

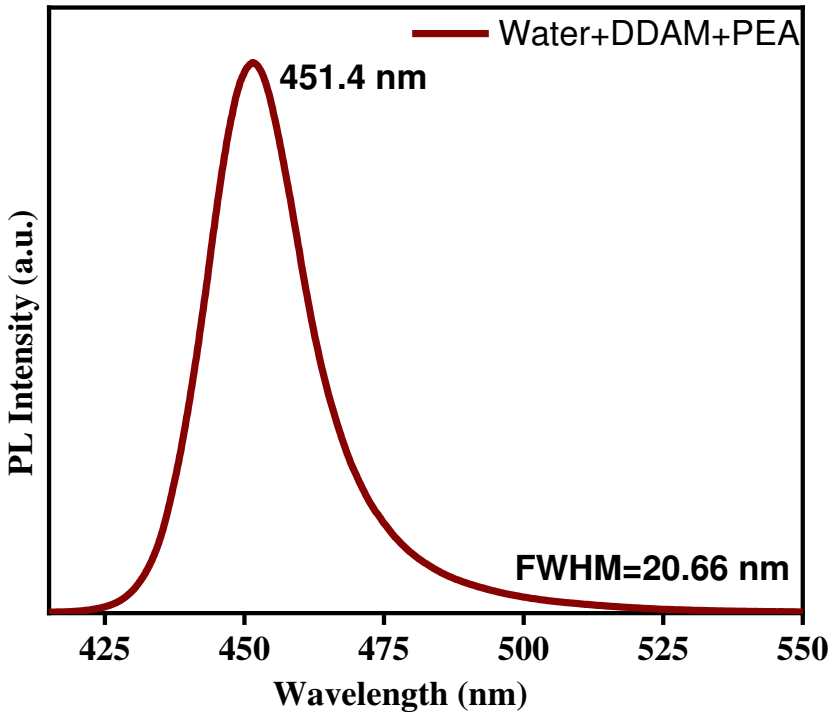

Figure S14. PL Intensity of the WD-synthesized with ligand exchange method.

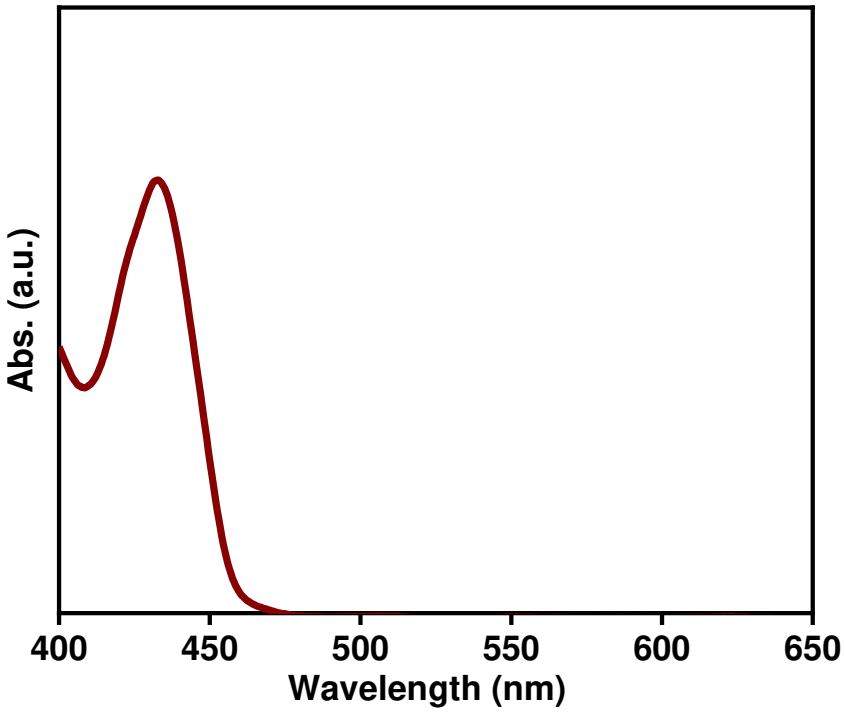

Figure S15. UV spectra of WD-synthesized QWs with ligand exchange method.

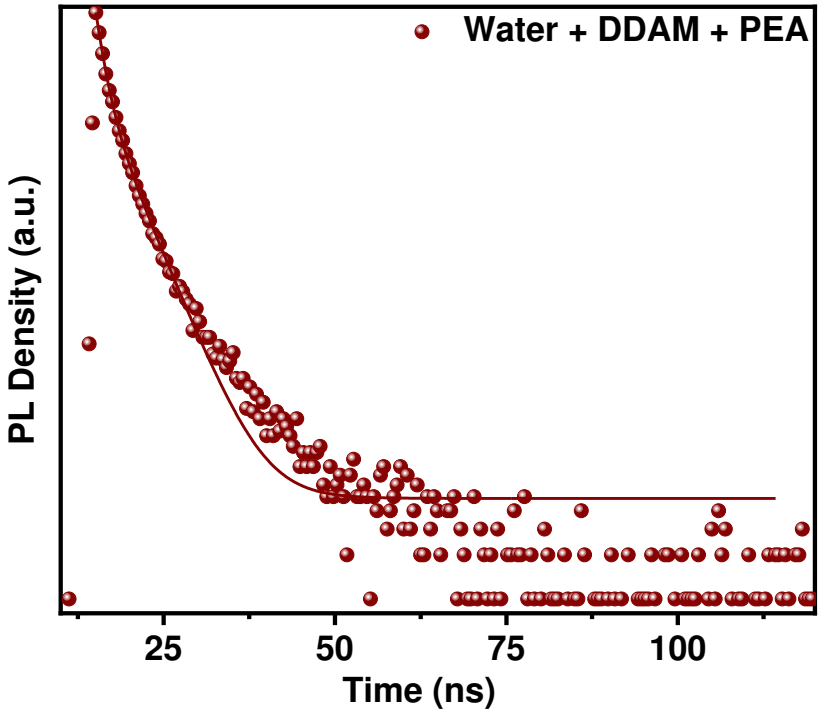

Figure S16. TR PL profile of the WD-synthesized QWs with ligand exchange method.

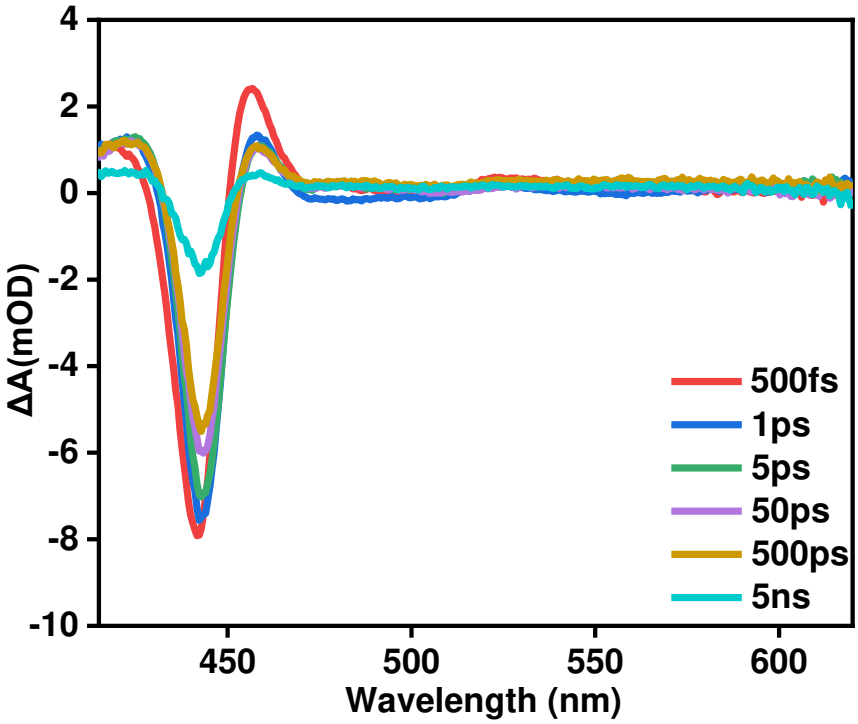

Figure S17. fs-TA spectra of the WD-synthesized QWs with ligand exchange method.

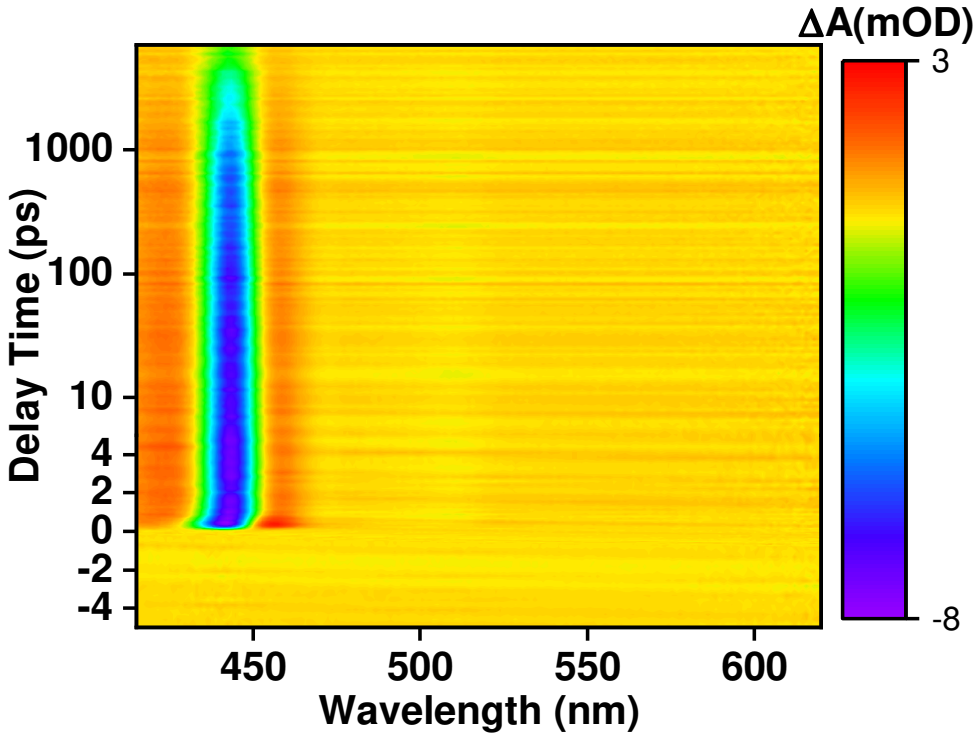

Figure S18. Pseudo-color plots of the WD-synthesized QWs with ligand exchange method.

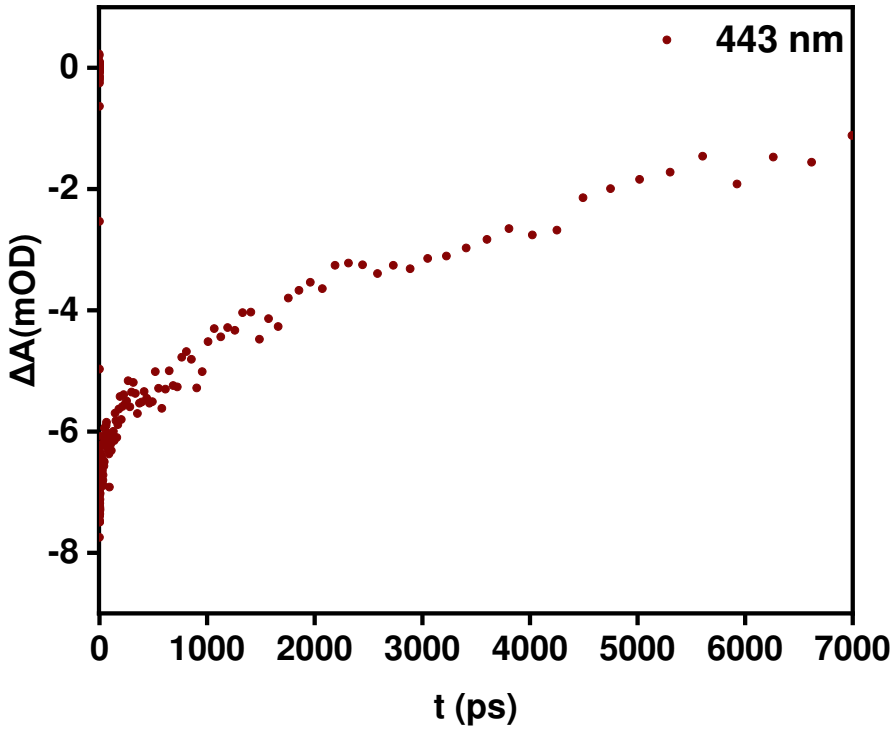

Figure S19. Blech recovery dynamics of the ligand-exchanged QWs.

Table S1. Optical performance including emission peak and FWHM of the WD-synthesized $CsPbBr_3$ QWs with addting water for 0s, 15s, 30s, 45s, and 60 s, respectively.

Water treatment period (s)	**0**	**15**	**30**	**45**	**60**
Emission Peak(nm)	459	459	460	458	462
FWHM (nm)	26.2	23.4	20.5	22.9	21.3

Table S2. Optical performance including emission peak and FWHM of the WD-synthesized $CsPbBr_3$ QWs with various water additive of 0 μL, 10 μL, 20 μL, 30 μL, 40 μL, 50 μL, 70 μL, and 90 μL, respectively.

Water Additive (μL)	**0**	**10**	**20**	**30**	**40**	**50**	**70**	**90**
Emission Peak(nm)	454.6	454.9	458	455.2	455	454	453.6	458.2
FWHM (nm)	30.5	26.8	25.9	24.4	24.8	25.2	24.52	22.2

Table S3. Summary of TA spectra fitting parameters for solutions of the pristine and WD-synthesized QWs.

	EMP	τ_1[ps]	τ_2 [ps]	A_1	A_2
Pristine	439	10.6 ± 0.7	1508.0 ± 137.5	-1.14 ± 0.03	-0.83 ± 0.03
WD-synthesized QWs	437	3437.80148±123.05279	-	-0.00299 ± 4.19528E-5	-

Table S4. Lifetime component of the pristine QWs.

Model	**ExpDecay3**
Equation	**y = y0 + A1*exp(-(x-x0)/t1) + A2*exp(-(x-x0)/t2) + A3*exp(-(x-x0)/t3)**
Plot	**Pristine QWs**
y0	2.03005 ± 0.9946
x0	3.90625 ± 0
A1	5014.89601 ± 221.65229
t1	0.66405 ± 0.01849
A2	4478.54853 ± 136.28401
t2	2.07313 ± 0.11017
A3	596.68359 ± 156.08099
t3	5.97918 ± 0.6312
Reduced Chi-Sqr	292.1733
R-Square (COD)	0.99963
Adj. R-Square	0.99963

Table S5. Lifetime component of the WD-synthesized QWs.

Model	ExpDecay2
Equation	**y = y0 + A1*exp(-(x-x0)/t1) + A2*exp(-(x-x0)/t2)**
Plot	**WD-synthesized QWs**
y0	3.84598 ± 0.60436
x0	5.17578 ± 0
A1	3011.59545 ± 58.4011
t1	1.62329 ± 0.02508
A2	3495.4911 ± 61.08726
t2	4.63009 ± 0.03879
Reduced Chi-Sqr	242.4697
R-Square (COD)	0.99963
Adj. R-Square	0.99962

Table S6. TR PL profile of water-driven ligand-exchanged QWs.

Model	ExpDecay2
Equation	**y = y0 + A1*exp(-(x-x0)/t1) + A2*exp(-(x-x0)/t2)**
Plot	**W+DDDAB+PEA**
y0	4.863 ± 1.44079
x0	15.13672 ± 0
A1	7034.80123 ± 110.90533
t1	1.11996 ± 0.01617
A2	3008.00506 ± 113.40756
t2	3.78496 ± 0.0801
Reduced Chi-Sqr	339.67802
R-Square (COD)	0.99968
Adj. R-Square	0.99968